The TOP counter of Belle II: status and first results

Umberto Tamponi, on behalf of the Belle II TOP group

INFN - Sezione di Torino, 10124 Torino

Abstract

High-efficiency and high-purity particle identification are fundamental requirements for the success of the Belle II experiment, whose main goal is to explore the new-physics scenarios in the CP-violating decays of B mesons. To achieve the required particle identification performances, the Time-Of-Propagation counter has been installed in the central barrel region. This unique device consists of 16 bars of fused silica that act simultaneously as radiator and as light guide for the Cerenkov light. Unlike in the DIRC detector, the particle identification is mostly performed by measuring the time of propagation of the Cherenkov light in the radiator rather than its purely geometrical patterns. We will present here a general overview of the status of the TOP counter, including the estimation of the time resolution, the calibration strategies and performances, and the first result obtained in the commissioning phase, both using cosmic rays and e^+e^- collision events collected during the *phase II* pilot run of the Belle II experiment. These are the first measurements of the particle identification performances of a time-of-propagation detector in a full HEP experimental setup.

Keywords: particle identification; BelleII; TOP; Cherenkov detectors;

1. Overview

The Belle II experiment [1] at the SuperKEKB collider aims to collect 50 ab^{-1} of e^+e^- collisions at the $\Upsilon(4S)$ and the nearby bottomonium resonances $\Upsilon(3S, 5S, 6S)$ to perform precision measurements of the rare B meson decay, search for signatures of new physics in the dark sector, and study the spectroscopy of exotic hadrons [2].

The first part of the data taking, the pilot run called *phase II*, started in April 2018 and lasted until July, collecting a total luminosity of about 0.5 fb^{-1}. All the sub-detectors were installed during the data taking except for the inner silicon tracker, that was almost completely replaced by beam-background monitoring sensors. Only one eighth of the inner tracker was installed for commissioning purposes. The phase II dataset has been used to commission the experiment, perform the early calibration and determine the initial performances of each sub-detector. In the following, we will discuss in detail the results of the commissioning of the Time-Of-Propagation (TOP) counter.

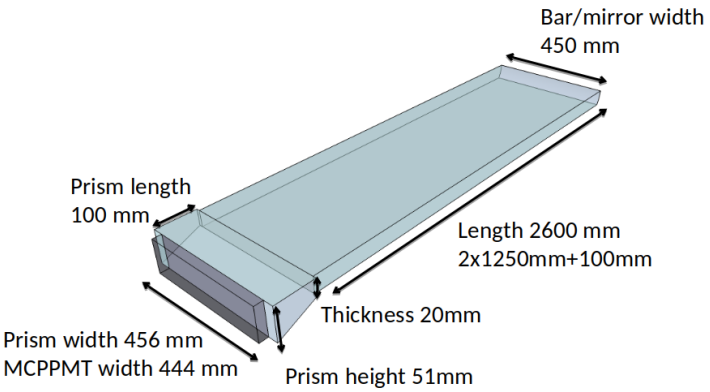

Figure 1: Sketch of one of the 16 modules of the TOP detector. The junctions between the two bar sections and between the bar and the mirror section are not shown.

2. The TOP counter

The TOP counter of the Belle II experiment is the only existing, operational time-of-propagation Cherenkov counter [3, 4, 5, 6], and *phase II* represented the first attempt to perform particle identification with such a device in a collider experiment. It is composed by sixteen identical modules as the one sketched in Figure 1, arranged around the interaction point in a barrel-like geometry. Each module is composed of four parts glued together: two fused silica bars of dimensions $(125 \times 45 \times 2)$ cm acting as the Cherenkov radiator, a mirror located at the forward end of the bar, and a 10 cm long prism that couples the bar with an array of micro-channel-plate photomultiplier tubes (MCP-PMTs) [7, 8]. Thanks to the high average refractive index ($n = 1.44$ at 405 nm) of the fused silica, part of the Cherenkov radiation emitted by the particles crossing the radiator remains trapped by total internal reflection, propagating to the MCP-PMT array. Having a pixel size of approximately 5.5×5.5 mm and a transit time spread less than 50 ps, the MCP-PMTs provide a coarse measurement of the photon positions and a very precise measurement of their detection time. The photo-electron detection time, measured with respect to the initial e^+e^- collision, can be decomposed into two con-

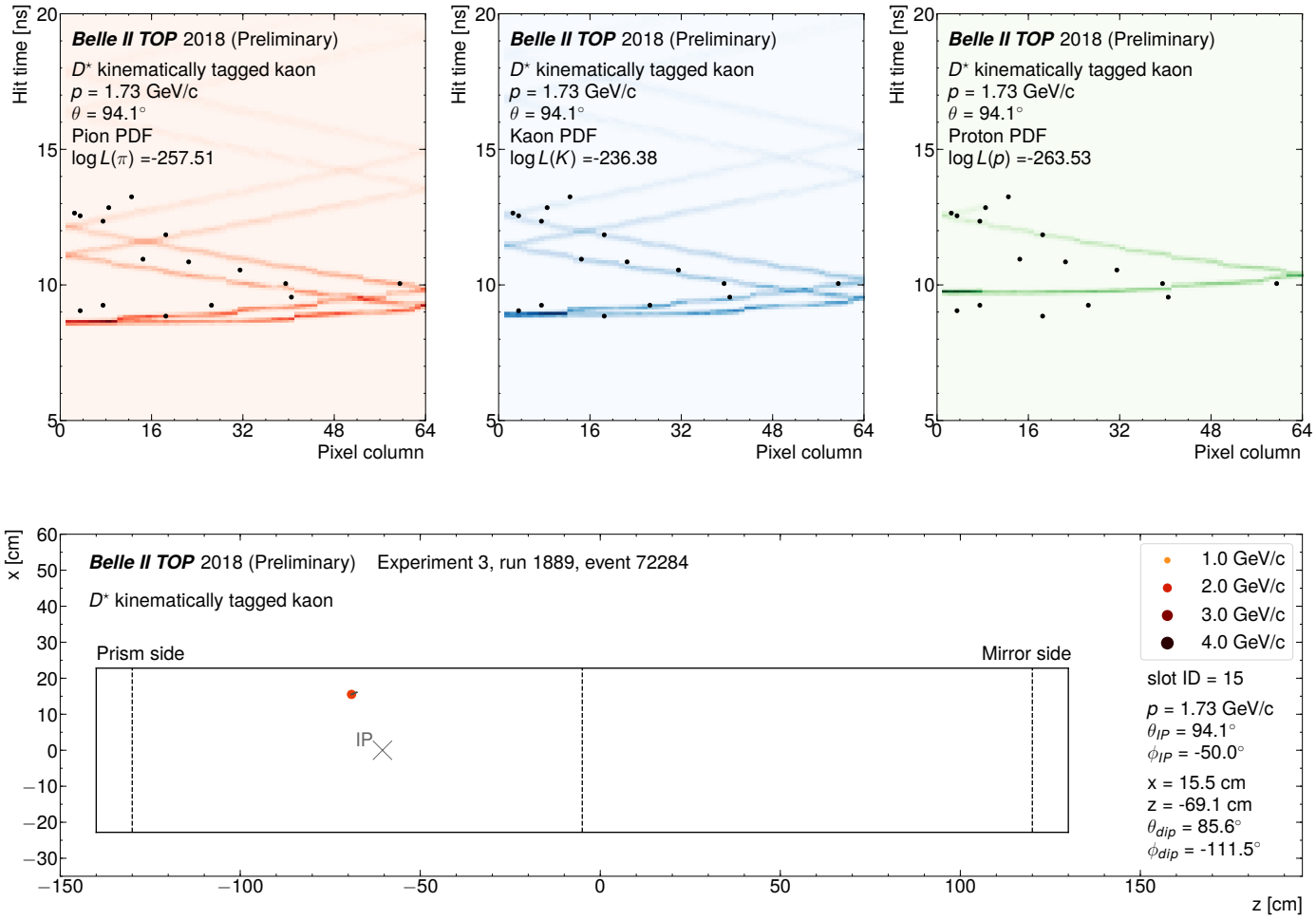

Figure 2: *Upper panels*: space-time distribution of the hits associated to a kaon candidate track selected in the phase II data. The x-axis represents the position of the pixel along the bar transverse dimension, while the y-axis represents the detection time, referred to the most probable bunch crossing. The black points represent the observed hits, while the smooth distribution the expected PDF for a pion (*upper left*), a kaon (*upper center*) or a proton (*upper right*) of same momentum. *Lower panel* : reconstructed position (red marker) and direction (black segment) of the kaon candidate at its entrance in the TOP active volume. The size of the marker is proportional to the track's momentum.

tributions: the time of flight of the charged particle from the interaction point to the TOP, and the time of propagation of the Cherenkov light inside the quartz. Once the direction of the incoming particle and the quartz optical properties are known, the latter is function only of the Cherenkov angle. The TOP therefore provides a combined measurement of both time of flight and Cherenkov angle.

The particle identification information is extracted by comparing the distribution of the time of arrival of the photons in each of the 512 channel with the expected Probability Density Functions (PDFs) for six particle hypotheses (e, μ, π,K, p, d) [9]. The six corresponding likelihood values are then stored, and their ratios are used to assign identification probabilities. MC simulations show that a kaon identification efficiency of 90% can be achieved while keeping the pion fake rate below 5% in the momentum region between 0.5 and 2 GeV/c [2].

3. First results using pure samples of kaons

The early run with the TOP was overall successful: the detector took part in more than 90% of the physics runs, with a 2.5% fraction of dead channels, and its particle identification capabilities were demonstrated for the first time.

The TOP particle identification capabilities have been tested by selecting pure samples of pions, kaons and protons reconstructed in the decay chains $D^{\star+} \to D^0\pi^+ \to K^-\pi^+\pi^+$, $K_s \to \pi^+\pi^-$, and $\Lambda \to p\pi^-$ [1]. We will focus on the kaon/pion separation power and on the pion fake rates, determined using the $D^{\star+}$ and the K_s decays in the first 90 pb^{-1} of data. All the results presented here have been obtained with preliminary, severely limited time calibrations and without any geometrical alignment. This prevents us from presenting here precise numerical results.

[1] Charge conjugation is understood for all the processes discussed in this paper.

The $D^{\star+}$ reconstruction begins with selecting the $D^0 \to K^-\pi^+$ candidates. The D^0 is reconstructed from track pairs of opposite charge pointing to the primary interaction point. The K mass hypothesis is assigned to one track and π one to the other one, without using any particle identification information. The kaon candidate is required to be within the TOP acceptance. After applying a kinematic fit to constrain the track to a common vertex, we discard most of the combinatorial background by requiring the D^0 candidate to have mass between 1.85 GeV/c^2 and 1.88 GeV/c^2, corresponding to a 2.5σ window around the D^0 peak. The remaining D^0 candidates are then combined with an additional track of charge opposite of the kaon to reconstruct the $D^{\star+}$ candidates. Again, we apply a vertex-constrained kinematic fit and we require the mass difference between the $D^{\star+}$ and the D^0 candidate to be between 143.6 MeV/c^2 and 147.6 MeV/c^2. Finally we further suppress the combinatorial background by requiring the $D^{\star+}$ candidates to have momentum in the center-of-mass frame greater than 2.5 GeV/c^2. The result of this procedure is a small, but pure sample of K with less than 5% contamination from other particles, mostly pions.

Using this pure kaon sample one can clearly visualize how the Cherenkov rings are reconstructed in a coordinate-time space by the TOP counter. Figure 2 shows the MCP-PMT hit timing distribution associated to a kinematically tagged kaon, compared with the PDFs expected for a pion, kaon or proton of the same momentum and angle.

For each kinematically tagged kaon, we calculate the likelihood values $\mathcal{L}_\pi$ and $\mathcal{L}_K$ for the pion and kaon hypotheses by comparing the observed time and spacial distribution of the detected photons with the expected ones. Figure 3 shows the log-likelihood difference $\Delta LL = \log \mathcal{L}_K - \log \mathcal{L}_\pi$. The distribution is shifted towards positive values, indicating that the TOP is more likely to identify kaons as kaons rather than pions, as expected.

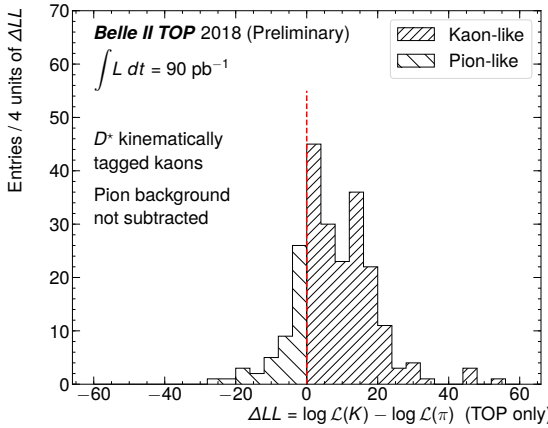

Figure 3: Difference between $\log \mathcal{L}_K$ and $\log \mathcal{L}_\pi$ for the kaons tagged by the $D^{\star+} \to D^0[\to K^-\pi^+]\pi^+$ decay. Only the TOP detector is used to calculate the likelihood values.

4. First results using pure samples of pions

To measure the probability $\mathcal{P}(\pi \to X)$ for a pion to be misidentified as another particle X, we reconstruct the $K_s \to \pi^+\pi^-$ decay, applying the same loose criteria used to select the tracks for the $D^{\star+}$ reconstruction. In addition, one of the two pions is required to be within the TOP acceptance (*probe*), while no selection is applied to the other track. We then study the yield of K_s as a function of the TOP response for the *probe* pion. Requiring $\log \mathcal{L}_X > \log \mathcal{L}_\pi$ we estimate $\mathcal{P}(\pi \to X)$, while to measure $\mathcal{P}(\pi \to \pi)$ we require $\log \mathcal{L}_\pi > \log \mathcal{L}_K$. The K_s mass distributions for four samples with different requirements on the likelihoods values are shown in Figure 4. As expected, the K_s peak is clearly suppressed when the *probe* track is more compatible with the either the K, p or e hypotheses rather then the π one.

Overall, the identification efficiencies for proton (not presented in this paper), kaon and pion measured in the commissioning run are approximately 10% below the Montecarlo expectations. Similar discrepancies are also present in the fake-rate measurement, which are higher than the design value. Numerous studies are being performed to better understand these differences and reduce or eliminate them, as discussed in the next section.

5. Understanding the performances

The early analysis of the phase II data points to the preliminary calibrations used to reconstruct the data as the primary cause of the reduced particle identification capability. The TOP calibration consists of a time calibration, whose aim is to even the response of the 8192 MCP-PMT channels, and a geometrical alignment. The time calibration is performed in four consecutive steps, each one depending on the previous ones [10]:

- Time-base calibration. This calibration aims to ensure the linearity of the front-end ASIC sampling array [11], and is performed by injecting electronic pulses in the front-end. After this calibration we measure, using a dedicated laser system [12], a single photo-electron time resolution per channel of approximately 120 ps.

- Channel T_0 calibration. Once the electronics has been properly calibrated, we compensate for the relative delays of the 512 channels within each TOP module. This calibration is performed by flashing the MCP-PMTs with a picosecond laser [12], and measuring the individual delay of each channel with respect to a reference channel.

- Geometrical alignment and module T_0 calibration. The laser calibration assures that all the delays within each module are properly compensated, but does not correct for the delays between modules (namely, the relative delays between the reference channels of each module). The synchronization of the modules is expected to be done together with the geometrical alignment by an iterative procedure based on di-muon events from e^+e^- collisions [10].

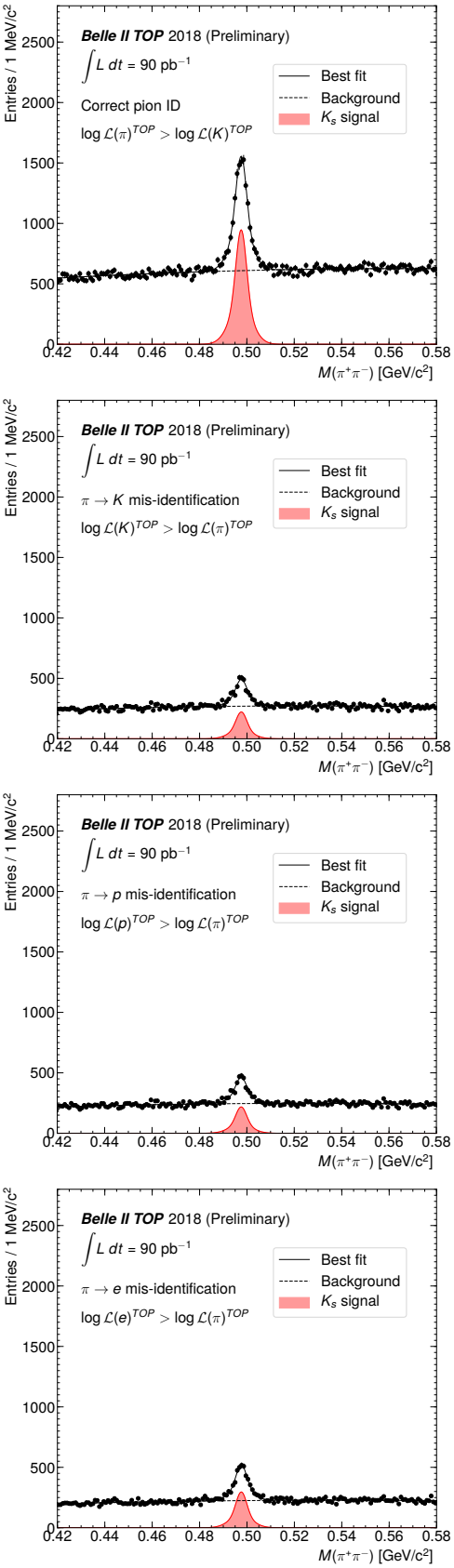

Figure 4: Mass distribution of the K_s candidates with four particle identification requirements. From top to bottom: $\log \mathcal{L}_\pi > \log \mathcal{L}_K$, $\log \mathcal{L}_K > \log \mathcal{L}_\pi$, $\log \mathcal{L}_p > \log \mathcal{L}_\pi$ and $\log \mathcal{L}_e > \log \mathcal{L}_\pi$.

- Global T_0. The Cherenkov photon time is measured with respect to the time of the original e^+e^- interaction. A very precise time reference is given by the accelerator Radio-Frequency (RF) clock, but to use it one needs to associate each event with the corresponding bunch crossing. This can be done by collecting all the particles detected in the event and, from the time of the hits in the TOP counter, fit the most probable interaction time. This algorithm has a resolution of $\approx$ 300 ps per event (to be compared with the SuperKEKB bunch crossing interval of 2 ns), corresponding to a bunch crossing identification efficiency greater than 95%. For this procedure to be successful, one needs to calibrate the delay between the RF clock and the TOP (or in other words, the relative phase) to a precision equal or smaller than the intrinsic uncertainty on the interaction time of 20 ps due to the bunches length. Any residual phase between the TOP and the RF clock will result in a net extra contribution to the TOP time measurement.

During and after the data taking, we found several issues in each of the above calibration steps. First, residual non-linearities that, despite being rather small, significantly reduced the precision of the laser calibration. Then, the statistics of di-muon collected is not sufficient to perform any of the track-based calibration to the required degree of precision. A first attempt to perform the geometrical alignment and module T_0 calibration was made but produced unreliable results due to the very limited $\mu^+\mu^-$ statistics. Since the time calibration of the modules with each other is critical for the TOP reconstruction, an alternative algorithm has been developed to use muons from the 2018 cosmic ray test dataset. The geometrical alignment has not been performed. The global T_0 calibration must be calculated for every run, but the statistics available still significantly limits its precision to $\approx$ 150 ps on an typical run, $\approx$ 300 ps for the shortest run and $\approx$ 30 ps for the longest. This is the largest contribution to the total time resolution of the TOP detector identified so far. All these effects, combined with a reduced hit reconstruction efficiency due to the early version the front-end firmware used during phase II, and convoluted with all the effects coming from the preliminary tracking calibration, would fully explain the performance degradation we observed. We'd like to remark that all these problems have known solutions, that will be implemented for the beginning of the Phase III operations, in spring 2019.

References

[1] T. Abe, et al., Belle II Technical Design Report`arXiv:1011.0352`.
[2] E. Kou *et al.* [Belle II Collaboration], arXiv:1808.10567 [hep-ex].
[3] M. Akatsu *et al.*, Nucl. Instrum. Meth. A **440**, 124 (2000).
[4] T. Ohshima, ICFA Instrum. Bull. **20**, 2 (2000).
[5] K. Inami, Nucl. Instrum. Meth. A **595**, 96 (2008).
[6] K. Inami, Nucl. Instrum. Meth. A766 (2014) 5–8.
[7] K. Inami, Physics Procedia 37 (2012) 683 – 690.
[8] K. Matsuoka, S. Hirose, T. Iijima, K. Inami, Y. Kato, Y. Maeda, R. Mizuno, Y. Sato, K. Suzuki, PoS PhotoDet2015 (2016) 028.
[9] M. Staric, Nucl. Instrum. Meth. A **639**, 252 (2011).
[10] M. Staric [Belle II TOP Group], Nucl. Instrum. Meth. A **876**, 260 (2017).
[11] D. Kotchetkov *et al.*, arXiv:1804.10782 [physics.ins-det].
[12] U. Tamponi, Nucl. Instrum. Meth. A **876**, 59 (2017).